Response of Human Retinal Microvascular Endothelial Cells to Influenza A (H1N1) Infection and the Underlying Molecular Mechanism

Shuo Yang,[1,2] Zixin Fan,[2] Xiaofeng Lu,[2] Hui Liu,[3] Ziying Zhou,[2] Hui Qi,[2] Jian Zeng,[2] Mianying Zheng,[2] Xuan Zou,[3] Shisong Fang,[3] and Guoming Zhang[2]

[1]Jinzhou Medical University, Jinzhou, Liaoning, China
[2]Shenzhen Eye Hospital, Jinan University, Shenzhen Eye Institute, Shenzhen, Guangdong, China
[3]Shenzhen Center for Disease Control and Prevention, Shenzhen, Guangdong, China

Correspondence: Guoming Zhang, Shenzhen Eye Hospital, Jinan University, Shenzhen Eye Institute, 18 Zetian Road, Futian District, Shenzhen 518040, China; zhangguoming@sz-eyes.com.
Shisong Fang, Shenzhen Center for Disease Control and Prevention, 8 Longyuan Road, Nanshan District, Shenzhen 518073, China; szcdcssf@aliyun.com.
Xuan Zou, Shenzhen Center for Disease Control and Prevention, 8 Longyuan Road, Nanshan District, Shenzhen 518073, China; zoux@wjw.sz.gov.cn.

SY and ZF contributed equally to this work.

Received: October 7, 2023
Accepted: January 3, 2024
Published: January 22, 2024

Citation: Yang S, Fan Z, Lu X, et al. Response of human retinal microvascular endothelial cells to influenza a (H1N1) infection and the underlying molecular mechanism. *Invest Ophthalmol Vis Sci.* 2024;65(1):38. https://doi.org/10.1167/iovs.65.1.38

Purpose. Whether H1N1 infection–associated ocular manifestations result from direct viral infections or systemic complications remains unclear. This study aimed to comprehensively elucidate the underlying causes and mechanism.

Method. TCID50 assays was performed at 24, 48, and 72 hours to verify the infection of H1N1 in human retinal microvascular endothelial cells (HRMECs). The changes in gene expression profiles of HRMECs at 24, 48, and 72 hours were characterized using RNA sequencing technology. Differentially expressed genes (DEGs) were validated using real-time quantitative polymerase chain reaction and Western blotting. CCK-8 assay and scratch assay were performed to evaluate whether there was a potential improvement of proliferation and migration in H1N1-infected cells after oseltamivir intervention.

Results. H1N1 can infect and replicate within HRMECs, leading to cell rounding and detachment. After H1N1 infection of HRMECs, 2562 DEGs were identified, including 1748 upregulated ones and 814 downregulated ones. These DEGs primarily involved in processes such as inflammation and immune response, cytokine-cytokine receptor interaction, signal transduction regulation, and cell adhesion. The elevated expression levels of CXCL10, CXCL11, CCL5, TLR3, C3, IFNB1, IFNG, STAT1, HLA, and TNFSF10 after H1N1 infection were reduced by oseltamivir intervention, reaching levels comparable to those in the uninfected group. The impaired cell proliferation and migration after H1N1 infection was improved by oseltamivir intervention.

Conclusions. This study confirmed that H1N1 can infect HRMECs, leading to the upregulation of chemokines, which may cause inflammation and destruction of the blood-retina barrier. Moreover, early oseltamivir administration may reduce retinal inflammation and hemorrhage in patients infected with H1N1.

Keywords: H1N1, HRMECs, inflammation, hemorrhage, exudation

Influenza A virus is primarily known for its propensity to affect the respiratory system in both humans and animals.[1] Because of its rapid transmission, it poses a serious threat to human and animal health. The extensive spread of this virus has presented significant challenges to public health, imposing a heavy burden on the quality of life of citizens, as well as social and economic development. Influenza A virus has two types of glycoproteins on its surface, hemagglutinin (H) and neuraminidase (N). Currently, 18 HA subtypes and 11 NA subtypes are known. Various influenza A virus subtypes are formed by different combinations of hemagglutinin and neuraminidase, such as H1N1, H2N2, H3N2, H5N1, and H7N9.[2–4] Research indicates that since the 2009 pandemic, H1N1 has caused symptoms, such as high fever, cough, sore throat, and generalized weakness. It can also lead to severe pneumonia, acute respiratory distress syndrome, respiratory failure, multiple organ damage, and even death.[5–7] Some patients have also exhibited H1N1-associated ocular manifestations, primarily related to vasculitis.[8–10] However, whether these are resulted from direct viral infections or systemic complications remains unclear. Research has found that influenza viruses can cause degeneration of retinal pigment epithelial cell,[11] which are a major component of the blood-retinal barrier.[12] There is limited research on whether influenza viruses can infect retinal endothelial cells, which are the main components of the blood-retinal barrier. Therefore we conducted relevant studies to investigate whether the H1N1 influenza virus could effectively replicate in human retinal microvascular endothelial cells (HRMECs) and further explore its pathogenic mechanism.

High-throughput RNA sequencing technology has been widely used in recent years and has proven invaluable for providing high-quality genomic references and revealing potential gene functions and interactions.[13,14] Therefore it can be used to study host-pathogen relationships and analyze the molecular mechanisms of host-pathogen interactions in detail. In the present study, we used RNA sequencing technology to examine the host immune response in HRMECs infected with H1N1. We collected cells at 24, 48, and 72 hours after infection for transcriptomic analysis, which was further validated using real-time quantitative polymerase chain reaction (RT-qPCR) and Western blotting, aiming to provide novel insights into the pathogenesis of H1N1 infection.

Material and Methods

Cell Culture and Viruses

HRMECs were obtained from Shenzhen Eye Hospital, Jinan University, Shenzhen Eye Institute, and Madin-Darby Canine Kidney (MDCK) cells and H1N1 were supplied by the Shenzhen Center for Disease Control and Prevention. HRMECs were cultured in endothelial cell basal medium-2 (EBM-2) supplemented with a series of growth factors, 2% fetal bovine serum, and 1% penicillin-streptomycin. MDCK were cultured in minimum essential medium (MEM) supplemented with 10% fetal bovine serum, and growth factors were not needed.[15] Both cell lines were incubated at 37°C and 5% CO2, with medium changed every day to ensure the majority of cells were in the logarithmic growth phase for experimentation. As described previously, H1N1 was propagated in a monolayer of MDCK and the viral titer was determined using the 50% tissue culture infective dose (TCID50) method.[16] The multiplicity of infection (MOI) used for infection was 0.1. All experiments involving H1N1 were conducted in a biosafety level 2 laboratory at the Shenzhen Center for Disease Control and Prevention.

H1N1 Infection of HRMECs and Sample Preparation

The HRMECs were first seeded in a six-well plate with a cell density of 1×10^6 cells per well. After seeding, the cells were infected with the H1N1 virus at a MOI of 0.1. The infected cells were then incubated for a duration of two hours at a temperature of 35°C. Subsequently, they were incubated with serum-free growth medium at a temperature of 35°C for the following timepoints: 24 hours, 48 hours, and 72 hours. Concurrently, cells treated with equal volumes of EBM-2 were used as controls. The TRIzol reagent was used for HRMECs lysis (Thermo Fisher Scientific, Waltham, MA, USA), and the cell lysate was used to isolate total RNA. Besides, the oseltamivir we used in our research is oseltamivir acid (here referred to merely as oseltamivir), which is the active metabolite of oseltamivir.

Generation of a cDNA Library and RNA Sequencing

The Bioanalyzer 2100 and RNA 6000 Nano LabChip Kit (50671511; Agilent Technologies, Santa Clara, CA, USA) were used to analyze total RNA. RNA samples of excellent quality were used to generate sequencing libraries, which were purified, fragmented, reverse-transcribed into cDNA, and subjected to PCR amplification. The libraries were sequenced with a 2×150 bp paired-end read length on an Illumina Novaseq 6000 platform (LC-Bio, Hangzhou, China).

Extraction of Clean Reads and Sequencing

Quality analysis of RNA sequencing was conducted using FastQC software (http://www.bioinformatics.bbsrc.ac.uk/projects/fastqc/). Subsequently, the clean reads were aligned to the reference genome using the HISAT2 package (version: hisat2-2.2.1; https://daehwankimlab.github.io/hisat2/). The clean reads were mapped to the reference genome (Ensembl_v107, https://ftp.ensembl.org/pub/release-107/fasta/homo_sapiens/dna/) to conduct gene expression analysis based on exon segments using the per million mapped reads method, ultimately preserving high-quality readings.

Identification and Enrichment Analyses

DESeq2 (https://bioconductor.org/packages/release/bioc/html/DESeq2.html) was used to analyze differentially expressed genes (DEGs) (between two samples, edgeR software (https://bioconductor.org/packages/release/bioc/html/edgeR.html) was used. The genes with the parameter of false discovery rate <0.05 and absolute fold change ≥2 were considered differentially expressed genes. Enrichment analyses were carried out to investigate gene ontology (GO) and Kyoto Encyclopedia of Genes and Genomes (KEGG) pathways. The GO enrichment analysis included three aspects: molecular function, cellular components, and biological processes.

In addition, we performed gene enrichment analysis using GSEA software (https://www.gsea-msigdb.org/gsea/index.jsp) and MSigDB (http://software.broadinstitute.org/gsea/msigdb) to determine whether specific genes exhibit significant differences in particular GO terms or KEGG pathways. In summary, we used the Signal2Noise normalization method to calculate gene expression variations and rank the genes.

Validation of DEGs Using RT-qPCR

To analyze mRNA expression, total cellular RNA was extracted using TRIzol reagent. Following that, reverse transcription was carried out using the RevertAid First Strand cDNA Synthesis Kit (Thermo Fisher Scientific) to generate cDNA.[17] Subsequently, qRT-PCR was performed. Representative DEGs (CXCL5, CXCL10, CXCL11, CCL5, TLR3, C3, IFNA1, IFNB1, IFNG, IFIH1, ISG15, STAT1, HLA, CASP1, and TNFSF10) were selected based on the sequencing results (Table). We used the $2^{-\Delta\Delta Ct}$ method to normalize the relative expression values of the candidate gene mRNAs to the relative expression value of GAPDH in each sample, allowing for a quantitative analysis.[18] Three biological replicates were used for each treatment group.

Cell Toxicity Assay

A mixture (density: 8×10^4 cells/mL) of HRMECs and each well of a 96-well plate was supplemented with culture medium, with 100 µL per well and incubated until 80% confluency was reached. Then, H1N1 infection was performed with a predetermined MOI of 0.1 based on preliminary experiments. An appropriate amount of viral

Table. Primer Sequences

Gene	Sequence
GAPDH	Forward primer: CAGGAGGCATTGCTGATGAT
	Reverse primer: GAAGGCTGGGGCTCATTT
CXCL5	Forward Primer: AGCTGCGTTGCGTTTGTTTAC
	Reverse Primer: TGGCGAACACTTGCAGATTAC
CXCL10	Forward Primer: GTGGCATTCAAGGAGTACCTC
	Reverse Primer: TGATGGCCTTCGATTCTGGATT
CXCL11	Forward Primer: GACGCTGTCTTTGCATAGGC
	Reverse Primer: GGATTTAGGCATCGTTGTCCTTT
CCL5	Forward Primer: CCAGCAGTCGTCTTTGTCAC
	Reverse Primer: CTCTGGGTTGGCACACACTT
TLR3	Forward Primer: TTGCCTTGTATCTACTTTTGGGG
	Reverse Primer: TCAACACTGTTATGTTTGTGGGT
C3	Forward Primer: GGGGAGTCCCATGTACTCTATC
	Reverse Primer: GGAAGTCGTGGACAGTAACAG
IFNA1	Forward Primer: GCCTCGCCCTTTGCTTTACT
	Reverse Primer: CTGTGGGTCTCAGGGAGATCA
IFNB1	Forward Primer: ATGACCAACAAGTGTCTCCTCC
	Reverse Primer: GGAATCCAAGCAAGTTGTAGCTC
IFNG	Forward Primer: TCGGTAACTGACTTGAATGTCCA
	Reverse Primer: TCGCTTCCCTGTTTTAGCTGC
IFIH1	Forward Primer: TCGAATGGGTATTCCACAGACG
	Reverse Primer: GTGGCGACTGTCCTCTGAA
ISG15	Forward Primer: CGCAGATCACCCAGAAGATCG
	Reverse Primer: TTCGTCGCATTTGTCCACCA
STAT1	Forward Primer: CAGCTTGACTCAAAATTCCTGGA
	Reverse Primer: TGAAGATTACGCTTGCTTTTCCT
HLA	Forward Primer: ACCCTCGTCCTGCTACTCTC
	Reverse Primer: CTGTCTCCTCGTCCCAATACT
CASP1	Forward Primer: TTTCCGCAAGGTTCGATTTTCA
	Reverse Primer: GGCATCTGCGCTCTACCATC
TNFSF10	Forward Primer: TGCGTGCTGATCGTGATCTTC
	Reverse Primer: GCTCGTTGGTAAAGTACACGTA

suspension was added to each well according to the known virus, TCID50, and incubated for 2 h. Afterwards, the plate was washed twice with an appropriate amount of 1 × PBS (Gibco, Grand Island, NY, USA). Three groups were established as follows: (1) medium without cells or test drugs, (2) medium containing cells without test drugs, and (3) medium containing cells and different concentrations of test drugs (0.1 nmol, 1 nmol, 10 nmol, 50 nmol, 100 nmol, 500 nmol, and 1000 nmol). After 24 hours of drug treatment, Mix CCK-8 (APExBio, Houston, TX, USA) and EBM-2 in a ratio of 1:9. For testing, each well received an addition of 100 µL mixture of CCK-8 reagent and EBM-2, which consists of 10 μl CCK-8 reagent and 90μL EBM-2, followed by incubation for two hours to allow the reaction to occur. The absorbance at 450 nm was measured to ensure the maximum nontoxic concentration of the drug. Three biological replicates were used for each treatment group.

Determination of the Optimal Drug Concentration

HRMECs were plated in 96-well plates with a density of 8×10^4 cells/mL. After approximately 24 hours of cell adherence, we administered appropriate treatments on the aforementioned groups of cells. After further incubation for 24 hours, the CCK8 experiment was conducted. After a two-hour incubation period, The absorbance at a wavelength of 450 nm was compared among different groups to determine the optimal drug concentration. Three biological replicates were used for each treatment group.

Western Blotting

After 24 hours of treatment, cells from the MOCK group, H1N1 group, and H1N1 + oseltamivir group were collected and used a protein extraction kit to extract total protein on ice (BB-319811-50T; Bestbio, Shanghai, China). The proteins were extracted based on the product manual. In brief, protease inhibitor and phosphatase inhibitor were added into precooled total protein extraction buffer in a ratio of 500:2:2. Cells were digested by 1 × 0.25% Trypsin-EDTA (Gibco) and washed twice with 1 × PBS (Gibco). For each cell group, 300 µL precooled total protein extraction mixture was added. After being shaken for 20 minutes to ensure complete cell lysis, the lysate was then transferred to a clean centrifuge tube and centrifuged at 12,000 × g for 15 min at 4°C. Finally, the supernatant was transferred to a pre-chilled clean centrifuge tube, yielding the total protein. The protein concentration was measured using an enhanced BCA protein assay kit (P0010; Beyotime, Shanghai, China). Subsequently, the protein was denatured by boiling and separated on an SDS-PAGE gel, followed by transfer onto a polyvinylidene difluoride membrane. The membrane was then blocked with a solution containing 5% skim milk at room temperature for two hours. The membranes were trimmed according to molecular weight and then incubated with primary antibodies against β-Actin (Cat no. 4967S, 1:1000; Cell Signaling Technology, Danvers, MA, USA), HLA (Cat no. 17260-1-AP, 1:1000; Proteintech, Rosemont, IL, USA), STAT1 (Cat no. 9172T, 1:1000; Cell Signaling Technology), TLR3 (Cat no. 6961S, 1:1000; Cell Signaling Technology), CXCL11 (Cat no. ab216157, 1:1000; Abcam, Cambridge, MA, USA), CXCL10 (Abcam; Cat no. ab306587, 1:1000), and C3 (Cat no. ab181147, 1:1000; Abcam) overnight on a shaker at 4°C. The membranes were washed three times with 1 × TBST (T1085; Solarbio, Beijing, China) at room temperature for 10 minutes each time and then incubated with an HRP-conjugated anti-rabbit secondary antibody (Cat no. SA00001-2, 1:3000; Proteintech), on a shaker at room temperature for two hours. The results were detected with super sensitive ECL substrate (BMU102-CN; Abbkine, Wuhan, China), with β-Actin antibody used as an internal reference.

Protein-Protein Interaction (PPI)

We systematically analyze the interactions between a large number of proteins through PPI[19] to gain insights into the functional connections between them. Proteins in living organisms do not exist independently; their normal functionality relies on the regulation by other proteins. In PPI analysis, highly clustered proteins may have similar or related functions. The network represents the connection between proteins, including those experimentally validated or predicted relationships, such as direct physical interaction, coexpression, and gene fusion.[20] In the analysis, different proteins are represented by nodes of different colors, and the thickness of the connecting lines indicates the degree of connectivity. Thicker lines represent stronger connections between the proteins on either side, indicating closely related protein relationships and providing potential candidates for further focused research.

Data Statistics and Analysis

Origin software (2021) is used for statistical analysis and visualization. The data obtained from TCID50, CCK8, RT-qPCR, and cell scratch testing were subjected to statistical analysis using a two-tailed unpaired Student's *t*-test. For omics analysis, R software was used with DESeq2 to perform DEGs between the two groups and edgeR used between the two samples. The data are shown as means ± SEM. All experiments were performed with at least three independent imaging or biological replicates. $P < 0.05$ is considered to be statistically significant (* $P < 0.05$,** $P < 0.01$, *** $P < 0.001$).

Results

H1N1 Infects HRMECs and Generate Active Progeny Viruses

To verify the successful infection of HRMECs with H1N1 and the production of active progeny viruses, a comparative experiment was conducted between the experimental and control groups (Fig. 1A). The TCID50 assay was performed on the viral supernatant at different time points to confirm successful infection of HRMECs. The results showed that H1N1 effectively replicated in HRMECs and generated infectious progeny viruses in a time-dependent manner (Fig. 1B). CCK8 assay revealed a noticeable decrease in cell viability at 24 hours after H1N1 infection (Fig. 1C). Changes in HRMECs morphology at 24, 48, and 72 hours after H1N1 infection are shown in Figure 1D, indicating cell rounding, detachment, and even cell death under microscopic observation.

Transcriptome Analysis of HRMECs Infected With H1N1

H1N1 was inoculated into HRMECs at an MOI of 0.1. Total cellular RNA was extracted using TRIzol reagent 24, 48, and 72 hours. RNA-seq was subsequently performed to examine the mRNA transcriptomes of H1N1-infected and control groups.

Transcriptomic analysis revealed that compared to the control group, the H1N1-infected group exhibited 884 upregulated genes and 499 downregulated genes at 24 hours, 479 upregulated genes and 217 downregulated genes at 48 hours, and 385 upregulated genes and 98 downregulated genes at 72 hours (Fig. 2A). In this study, a total of 2562 DEGs were identified, with 1748 genes showing upregulation and 814 genes showing downregulation. The heat map displays the fold-changes in DEGs between the two different treatment groups at 24, 48, and 72 hours (Fig. 2B).

GO analysis indicated that the DEGs in the control and H1N1-infected groups at 72 hours were abundantly concentrated in processes such as inflammation, signal transduction, and the immune response (Fig. 3A). PPI analysis of the DEGs enriched in the inflammatory process revealed a strong correlation between CXCL5, CXCL10, CXCL11, CCL5, TLR3, and C3 (Fig. 3B). KEGG pathway analysis demonstrated significant enrichment of DEGs in cytokine-cytokine receptor interaction, cell adhesion, and metabolic pathways in the H1N1-infected groups at 72 hours compared to the controls (Fig. 3C).

Venn analysis of DEGs at 24, 48, and 72 hours in H1N1-infected HRMECs revealed 169 upregulated and 12 downregulated genes (Fig. 4A). PPI analysis is shown in Figure 4B. PPI analysis of the commonly upregulated genes enriched in the inflammatory response pathway revealed close correlations between CCL5, TLR3, C3, CXCL11, and CXCL10, with the highest number of connections observed for CXCL10 (Fig. 4C). PPI analysis of DEGs enriched in the type II interferon signaling pathway revealed strong correlations among IFNB1, ISG15, STAT1, and HLA, with the highest number of connections observed for STAT1 (Fig. 4D). PPI analysis of the DEGs enriched in the cytokine response pathway indicated correlations between CXCL11, CXCL10, CASP1, CCL5, ISG15, TLR3, IFNB1, and HLA (Fig. 4E).

Total cellular RNA was obtained from control and H1N1-infected HRMECs at the three time points mentioned earlier. RT-qPCR was conducted to evaluate the relative mRNA expression levels of the identified DEGs, as shown in Figures 5A through 5O.

The analysis revealed a significant upregulation of CXCL5, CXCL10, CXCL11, CCL5, TLR3, C3, IFNA1, IFNB1, IFNG, IFIH1, ISG15, STAT1, HLA, CASP1 and TNFSF10 after infection. These results validate the findings of the transcriptomic analysis.

Oseltamivir Effectively Inhibits HRMECs Alterations Induced by H1N1

The maximum nontoxic concentration of oseltamivir (100 nmol/L) was determined using the CCK-8 assay, as shown in Figure 6A. Further experiments were conducted to determine optimal drug concentrations, which was 1 nmol/L (Fig. 6B) when different concentrations of the drug were applied to HRMECs infected with H1N1. The cellular morphology of the control group, H1N1-infected group, and H1N1-infected group treated with oseltamivir was observed at 24 hours, as shown in Figure 6C. Microscopic observations revealed a large amount of cell death after H1N1 infection, whereas cellular conditions significantly improved with oseltamivir intervention. Besides, the impaired migration ability in H1N1-infected cells was also improved after oseltamivir intervention (Figs. 6D, 6E).

RT-qPCR validation (Figs. 7A–7O) demonstrated that CXCL5, CXCL10, CXCL11, CCL5, TLR3, C3, IFNA1, IFNB1, IFNG, IFIH1, ISG15, STAT1, HLA, CASP1, and TNFSF10 were significantly upregulated after infection. However, with oseltamivir treatment, except for IFNA1, the expression levels of the aforementioned genes exhibited varying degrees of downregulation. In particular, CXCL10, CXCL11, CCL5, TLR3, C3, IFNB1, IFNG, STAT1, HLA, and TNFSF10 were downregulated to levels similar to those in the control group. These findings demonstrate that oseltamivir can effectively counteract the upregulation of chemokines and cell damage in HRMECs caused by H1N1.The results of WB were consistent with those of RT-qPCR (Fig. 8).

Discussion

Patients infected with H1N1 primarily exhibit symptoms such as fever, cough, muscle pain, fatigue, and respiratory distres.[21,22] Ocular manifestations in these patients include conjunctivitis, retinal lesions, retinitis, vasculitis, and serous chorioretinopathy.[23–26] In severe cases, it can progress to macular edema with significant exudation and subretinal hemorrhage,[27,28] eventually leading to visual impairment.[29] These pathological changes primarily affect the retinal vascular system and are characterized by extensive retinal hemorrhage and inflammatory exudation. However, the exact mechanism underlying these changes remains unclear. It is uncertain whether the virus directly infects the retinal cells or whether ocular complications result from a systemic disease. We have established for the

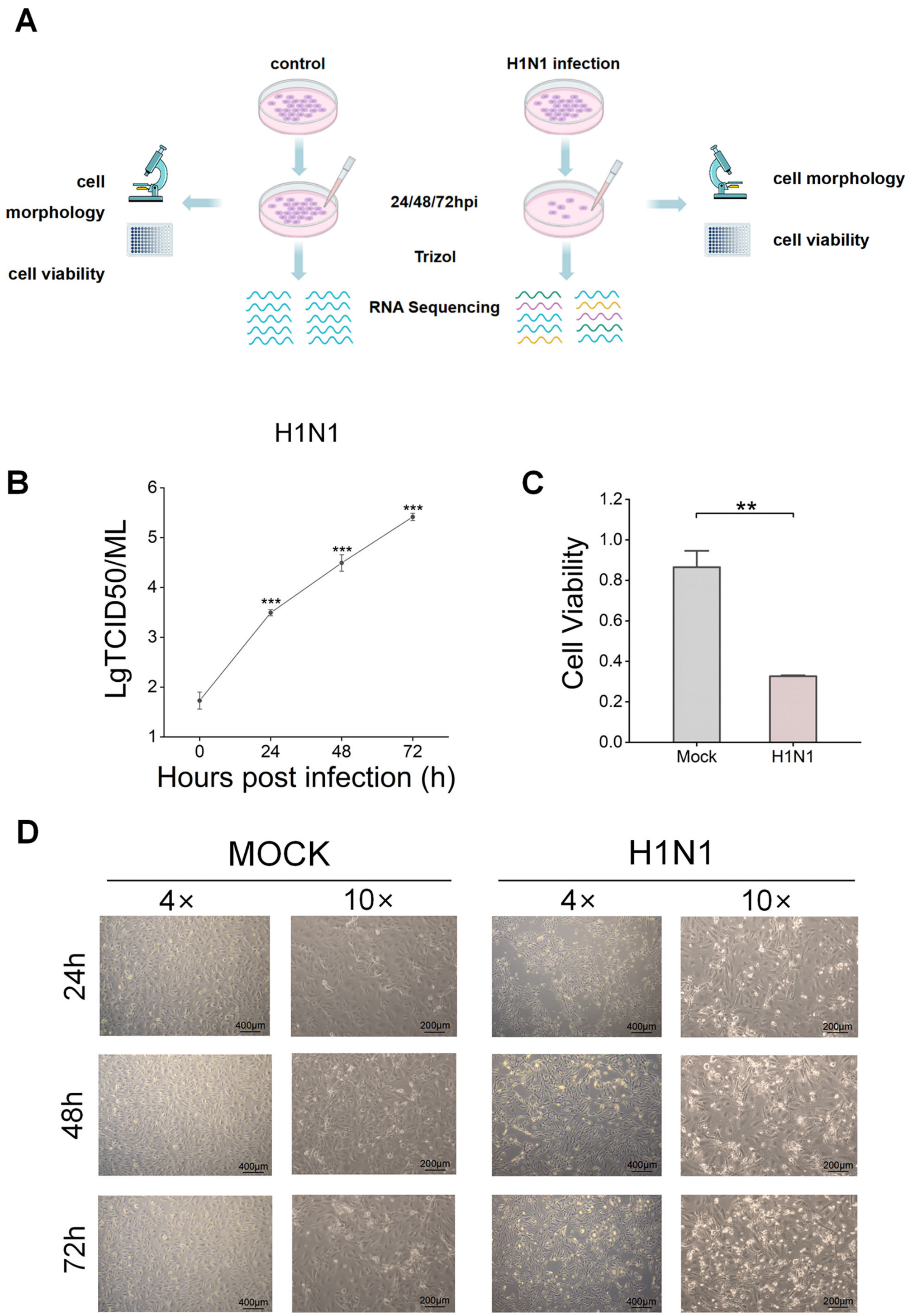

Figure 1. Experimental Scheme and H1N1 Infection of HRMECs. (**A**) HRMECs were mocked or infected with H1N1 (MOI = 0.1). Samples were collected at 24, 48, and 72 hours, and each group was prepared for total RNA extraction and sequencing (n = 3). (**B**) Amplification curve showing the increase in H1N1 titers in the cell culture supernatant of HRMECs. (**C**) CCK8 assay assessing the cell viability of HRMECs infected with H1N1 for 24 hours. (**D**) Morphology of HRMECs infected with H1N1 at 24, 48, and 72 hours.

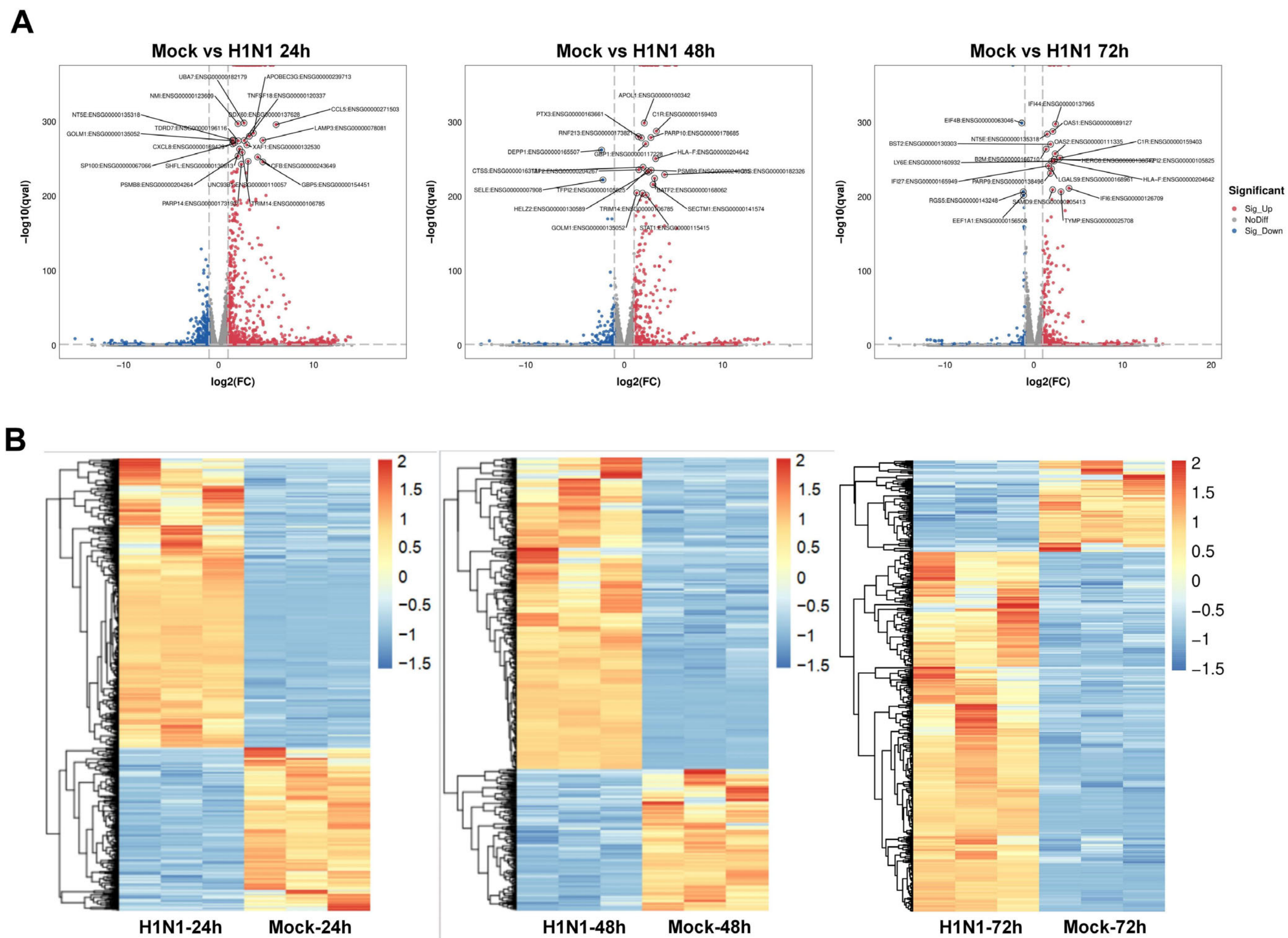

Figure 2. The DEGs in HRMECs infected with H1N1 (n = 3). (**A**) Volcano plots displayed the DEGs between H1N1 and control group at 24, 48, and 72 hours, with *red* indicating upregulation and *blue* indicating downregulation. (**B**) Heatmap showing the fold change of DEGs at 24, 48, and 72 hours, between the H1N1-infected and H1N1-uninfected groups.

first time that H1N1 can infect HRMECs and generate and release active progeny viruses. We have used transcriptomic techniques to analyze the alterations in the levels of gene expression across the entire genome after H1N1 infection in HRMECs and have validated these findings. This study aimed to explore the molecular mechanisms underlying H1N1-associated retinal lesions.

According to the transcriptome sequencing results, we detected 2562 DEGs between the infected and uninfected samples at various time points (24, 48, and 72 hours). Among these DEGs, 1748 genes were upregulated, and 814 genes were downregulated. These DEGs primarily participated in processes related to the regulation of signal transduction, immune system processes, cell adhesion, cytokine-cytokine receptor interactions, and inflammatory responses. Involvement in inflammation, type II interferon (IFN) signaling, and cytokine responses of the DEGs revealed noticeable alterations in the expression of numerous important chemokine and cytokine genes. As shown in Figure 5, Many chemokines (CXCL5, CXCL10, CCL5, and CXCL11) and interferon signaling pathway-related factors (IFNA1, IFNB1, and IFNG) were significantly upregulated after H1N1 infection, indicating the induction of strong inflammatory responses and signal transduction processes by H1N1.

During viral infection, immune cells produce large amounts of cytokines, which can both play an immunoregulatory role and trigger excessive immune responses. Therefore, if cytokines are not cleared in a timely manner after exerting their effects, it can lead to overactivation of inflammation, resulting in the production of excessive inflammatory factors and chemical mediators, which is referred to as a cytokine storm.[30] Cytokine release and clearance are complex regulatory processes. Numerous important molecular signaling molecules, such as cytokines and chemokines, play crucial roles in immune responses, inflammation, and certain pathological processes. These molecules mediate intercellular communications, regulate immune and inflammatory responses, and promote cell proliferation and differentiation.[31,32] Chemokines can guide cell migration in specific directions in tissues and play important regulatory roles in immune and inflammatory responses.[33] After H1N1 viral infection, the expression of chemokines, such as CXCL5, CXCL10, CXCL11, and CCL5, was significantly upregulated in HRMECs. CXCL5 enhances the activation, chemotaxis, and adhesion capacity of neutrophils, promoting neutrophil infiltration and inflammatory reactions at the site of inflammation.[34] Both CXCL10 and CXCL11 can attract specific immune cells, such as macrophages and

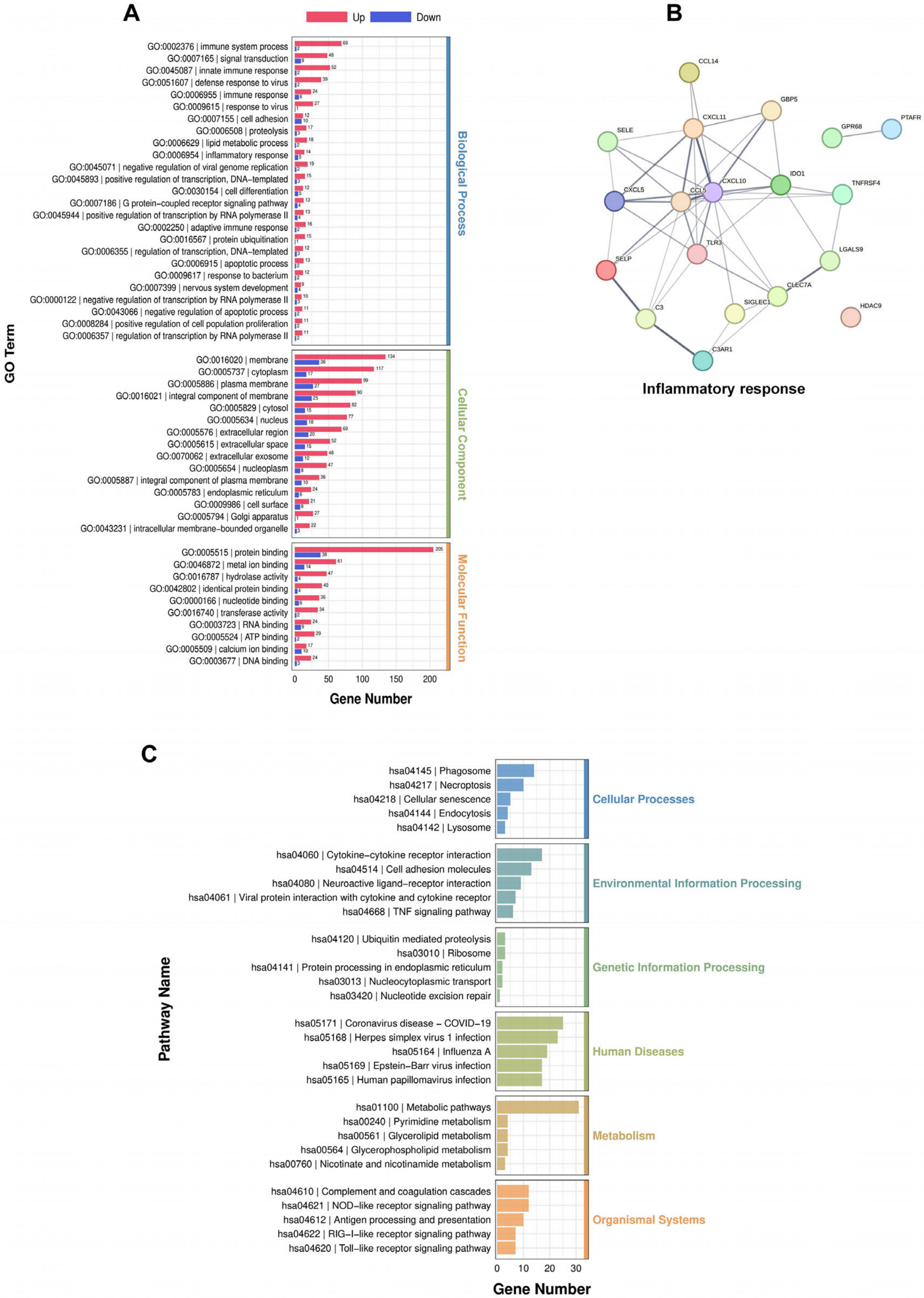

Figure 3. GO annotation and KEGG pathway enrichment analysis of DEGs in HRMECS infected with H1N1 virus, and the related PPI analysis.(**A**) Results of GO analysis, revealing the significantly enriched GO terms (top 50) in the DEGs between the mocked and H1N1-infected groups at 72 hours. (**B**) PPI analysis of DEGs at 72 hours that are significantly enriched to the inflammatory response. Different proteins are represented by different nodes and the thickness of the connecting lines indicates the degree of connectivity. (**C**) KEGG pathway analysis of significantly enriched DEGs between the mocked and H1N1-infected groups at 72 hours.

Investigative Ophthalmology & Visual Science

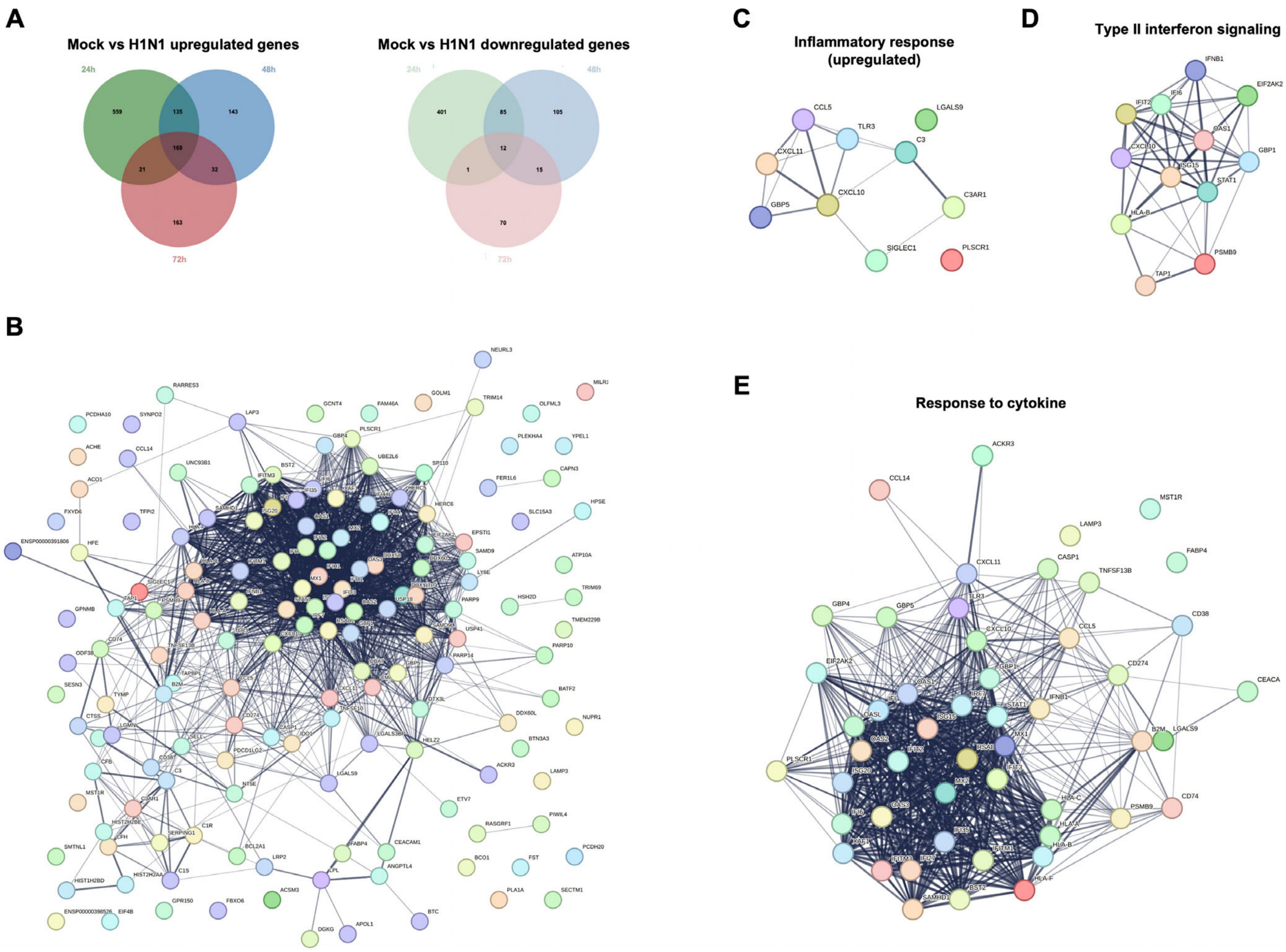

Figure 4. Venn analysis and the related PPI analysis. (**A**) Venn analysis was conducted to identify the common DEGs by H1N1 at 24, 48, and 72 hours. The analysis revealed a total of 169 upregulated genes and 12 downregulated genes. (**B**) PPI analysis that investigated the interactions between DEGs. (**C**) PPI analysis of the co-regulated DEGs that were enriched to inflammatory response. (**D**) PPI analysis of the coregulated DEGs that were enriched to Type II interferon signaling. (**E**) PPI analysis of the coregulated DEGs that were enriched to the response to cytokine. In PPI analysis, different proteins are represented by different nodes and the thickness of the connecting lines indicates the degree of connectivity.

natural killer cells, to actively move toward sites of inflammation.[35,36] CCL5 can facilitate the release of proinflammatory factors such as cytokines, chemokines, and lysosomal enzymes, further enhancing the activity of immune cells and inflammatory processes.[37] Studies have shown that these chemokines are often used to assess the extent of inflammatory reactions, investigate the occurrence and development of diseases, and evaluate the efficacy of drug treatments.[38] Therefore disease-related chemokines are potential therapeutic targets. This further supports the findings of our study, in which CXCL5, CXCL10, CXCL11, and CCL5, among other chemokines, were upregulated to varying degrees in HRMECs after H1N1 infection. This indicates that the H1N1 influenza virus can replicate rapidly and extensively within HRMECs, leading to overactivation and disruption of the immune system, ultimately resulting in the release of a large number of inflammatory factors.

IFN-related pathways play a crucial role in immune regulation and defense against viruses because they can activate immune cells to eliminate pathogens and promote immune responses. These are considered key pathways in the immune system and inflammatory responses.[39] When the body is infected with a virus, the virus invades host cells and begins to replicate. Infected cells initiate the synthesis and release of IFNs, which are secreted into the extracellular space and bind to their corresponding receptors, further activating signal transduction pathways and immune cells to enhance their ability to clear the virus.[40] IFNA1, IFNB1, and IFNG, the major members of the IFN family, exert antiviral effects during viral infections. IFNA1 and IFNB1 can enhance the activity of immune cells such as natural killer cells and macrophages, thereby improving their recognition and killing capacity against pathogens. Additionally, they stimulate the expression of antiviral genes to inhibit viral replication and transmission.[41–43] Despite being an inflammatory cytokine, IFNG can suppress the activity of inflammatory cells and exert anti-inflammatory effects in certain situations, thereby helping the body maintain an inflammatory balance. As demonstrated in Figures 5G through 5I, we confirmed the significant upregulation of IFNA1, IFNB1, and IFNG by RT-qPCR, indicating the activation of IFN-related pathways after H1N1 infection in HRMECs. As shown in Figure 4D,

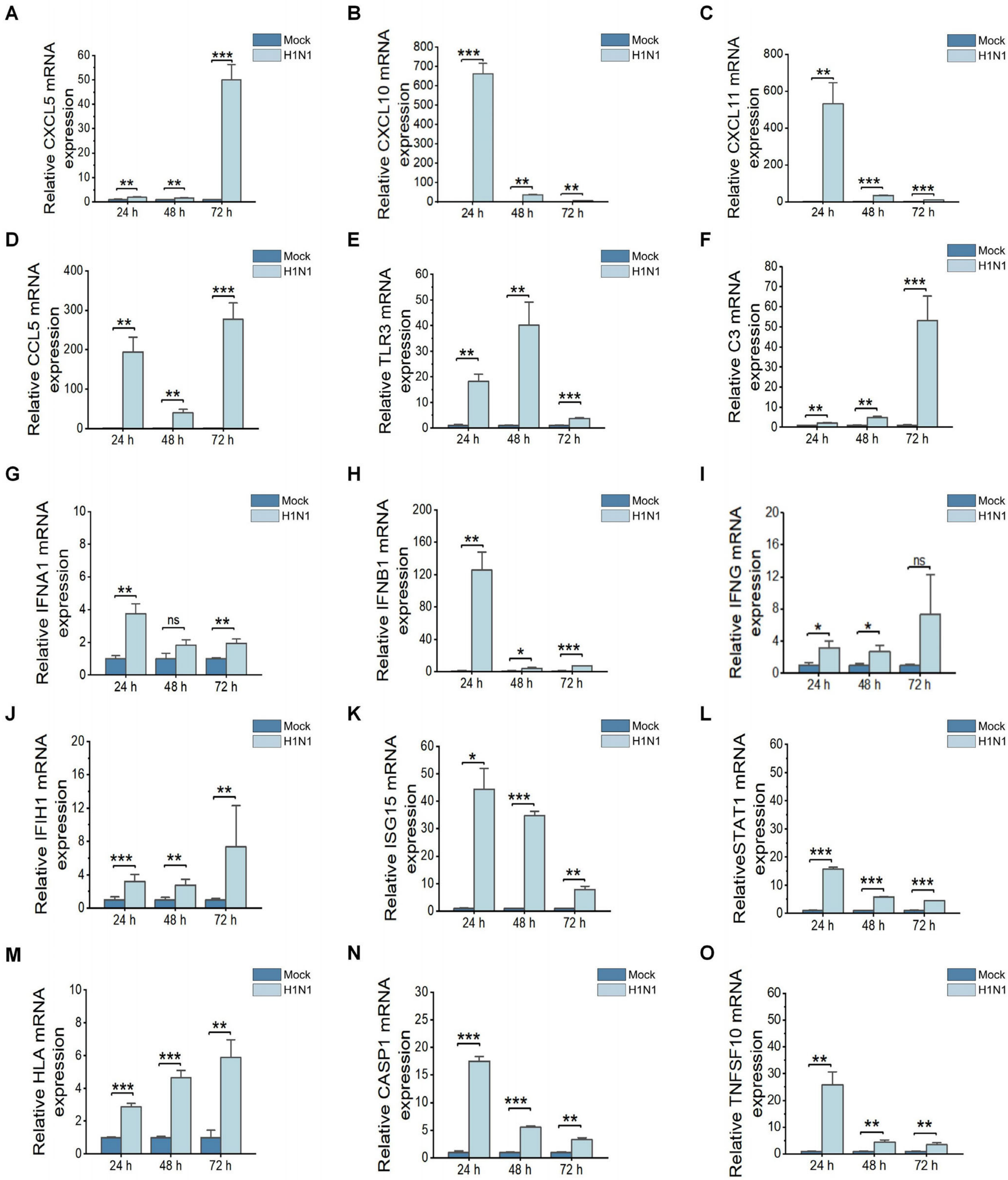

Figure 5. Representative DEGs involved in the mocked group and infected group of HRMECs were validated by RT-qPCR at 24, 48, and 72 hours (**A–O**). The resulting bar graph illustrates the expression levels of representative genes in HRMECs. The genes analyzed include CXCL5 (**A**), CXCL10 (**B**), CXCL11 (**C**), CCL5 (**D**), TLR3 (**E**), C3 (**F**), IFNA1 (**G**), IFNB1 (**H**), IFNG (**I**), IFIH1 (**J**), ISG15 (**K**), STAT1 (**L**), HLA (**M**), CASP1 (**N**), and TNFSF10 (**O**).

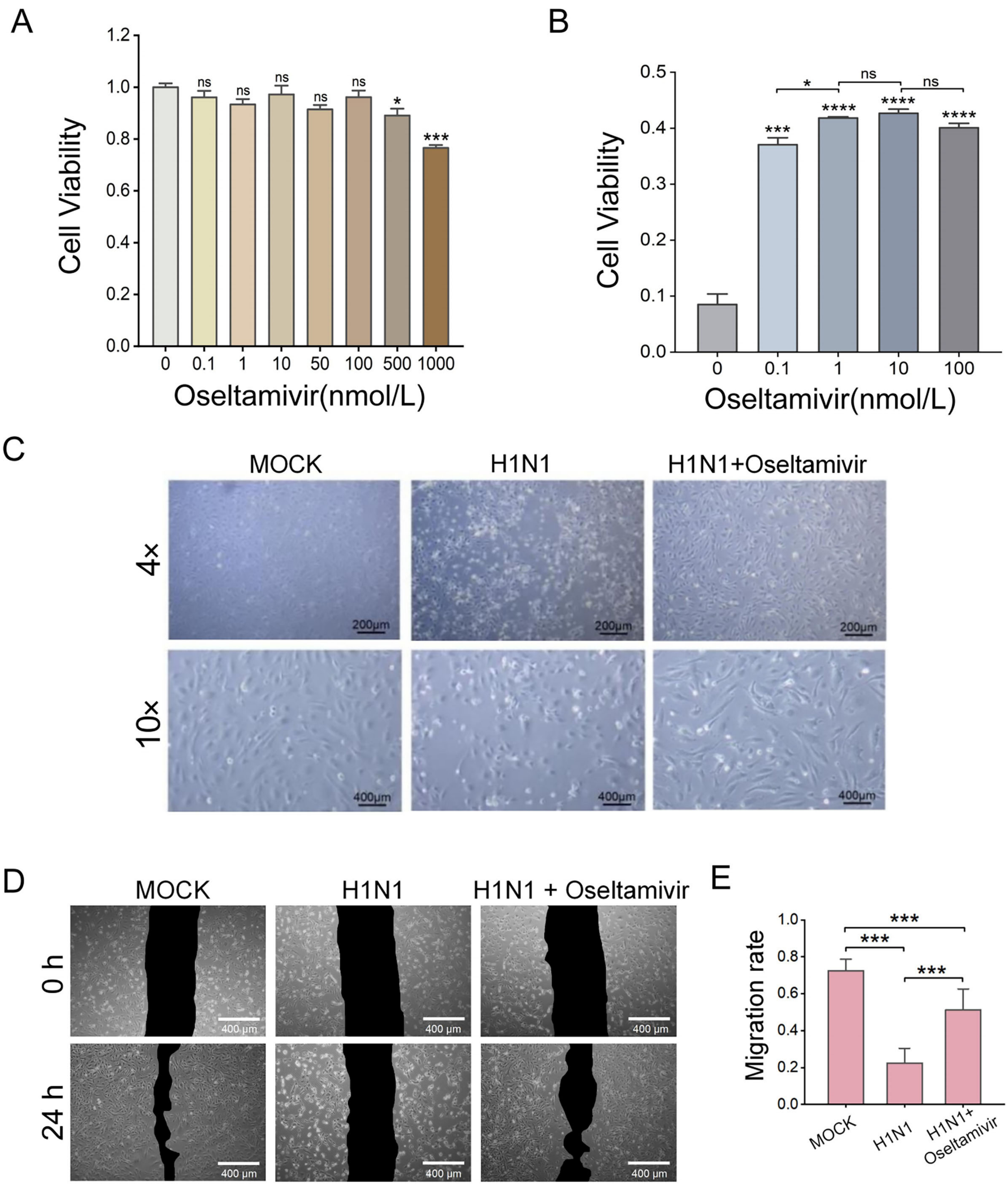

Figure 6. H1N1 inhibits the proliferation and migration of HRMECs, and oseltamivir can counteract the inhibitory effect of H1N1. (**A**) CCK-8 assay to assess toxicity of oseltamivir. (**B**) The selection of the optimal concentration of oseltamivir. (**C**) The effective inhibition of H1N1 infection in HRMECs by oseltamivir. (**D**) Representative scratch wound contrast photographs and measurement of wound area (area in between the two lines) over 24 hours. (**E**) The migration ability of HRMECs significantly decreases after being infected with H1N1.

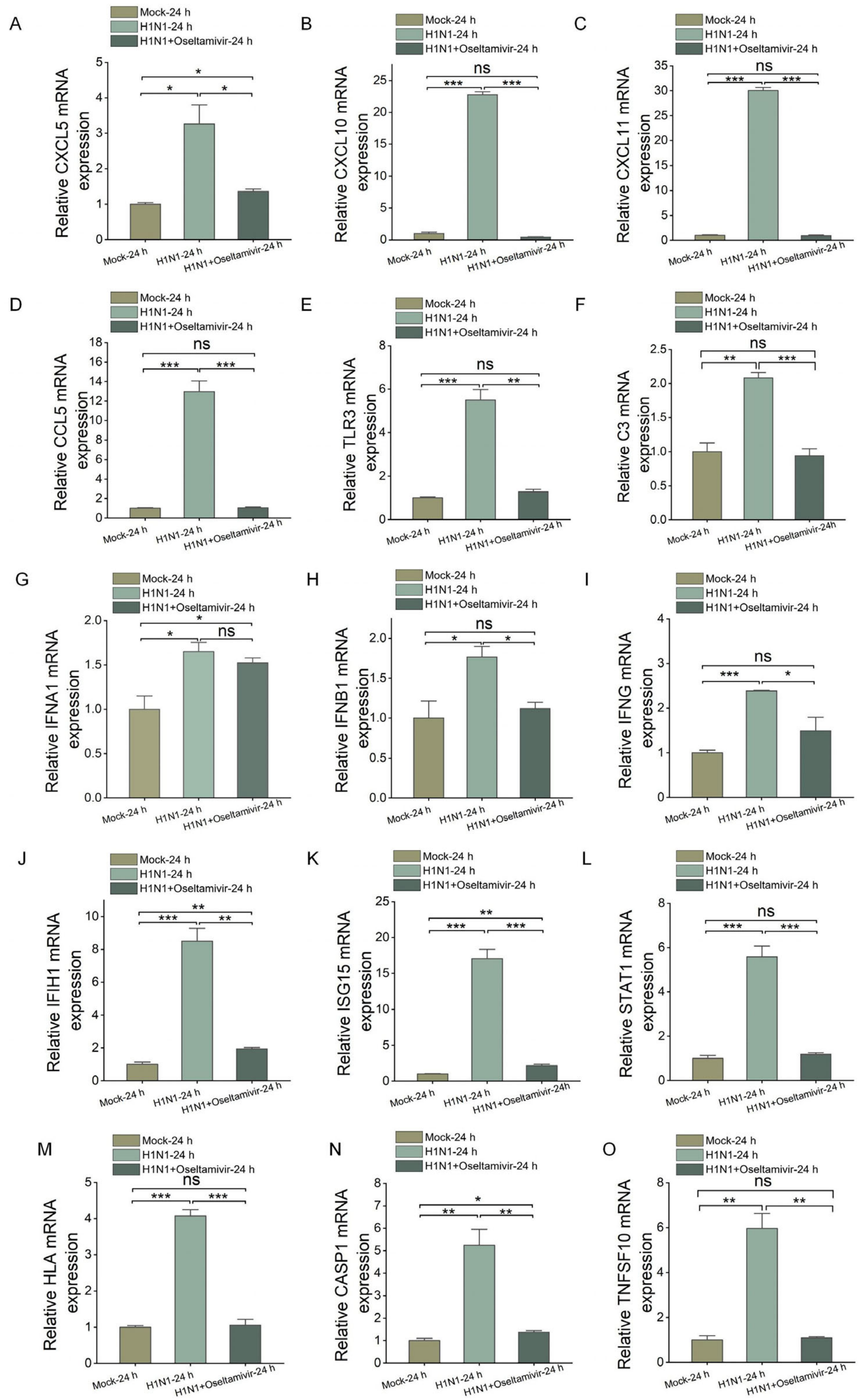

FIGURE 7. Validation of representative DEGs involved in H1N1 infection and early oseltamivir intervention by RT-qPCR at 24 hours (**A–O**). The bar graph represents the expression levels of representative genes in HRMECs through RT-qPCR. This includes (**A**) CXCL5, (**B**) CXCL10, (**C**) CXCL11, (**D**) CCL5, (**E**) TLR3, (**F**) C3, (**G**) IFNA1, (**H**) IFNB1, (**I**) IFNG, (**J**) IFIH1, (**K**) ISG15, (**L**) STAT1, (**M**) HLA, (**N**) CASP1, and (**O**) TNFSF10. Three groups of HRMECs were involved, including mocked, infected with H1N1, and infected with H1N1 and treated with oseltamivir.

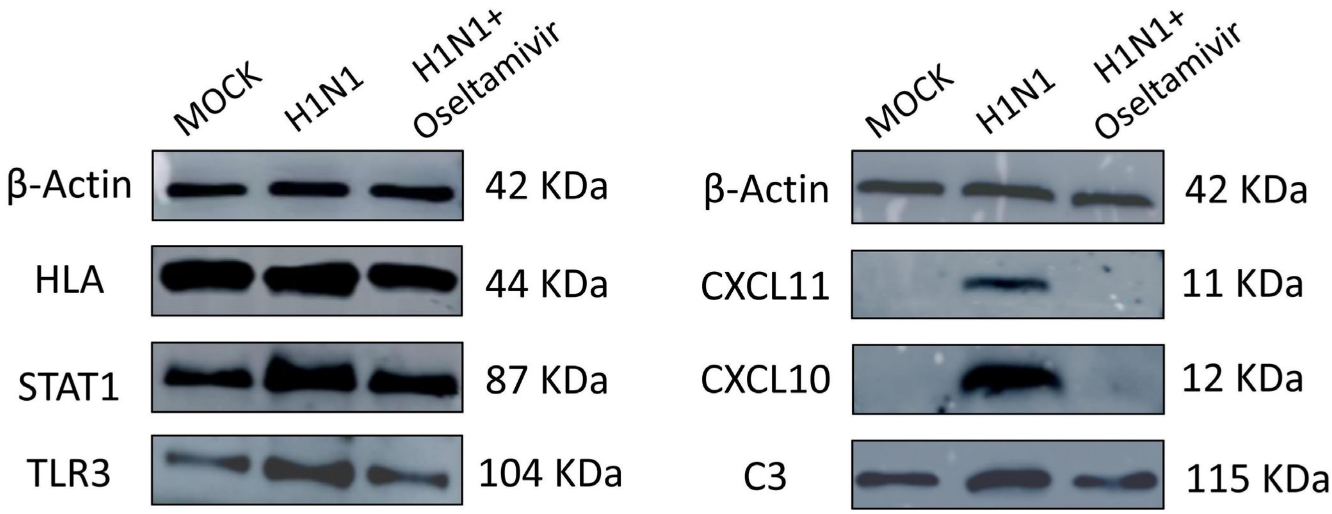

Figure 8. Representative images of Western blot. Western blot was used to detect the expression of HLA, STAT1, TLR3, CXCL11, CXCL10, and C3 in cells from the MOCK group, H1N1 group, and H1N1 + oseltamivir group. β-Actin was conducted as internal control gene.

analysis of the transcriptome sequencing results revealed that the DEGs were highly enriched in the pathway of type II IFN signaling. When the type II IFN receptor binds to type II IFN, endogenous tyrosine kinases (JAK) are activated. Activated JAK phosphorylates the IFN receptor, IFN-γR1, which further activates STAT proteins. Phosphorylated STAT proteins are transported to the nucleus to participate in the transcription of specific genes that encode a series of proteins that regulate immune and inflammatory responses, thereby defending the body against pathogen damage.[44] As shown in Figure 4B, PPI analysis of DEGs in this pathway revealed that the most tightly connected gene is STAT1. STAT1 is involved in intracellular signaling pathways and plays a crucial role in cellular immune responses and inflammation.[45] After stimulation by IFNs, STAT1 is activated and translocates into the cell nucleus to regulate the transcription and expression of multiple genes.[46] It not only possesses antiviral properties but also has the ability to activate other immune cells, thereby triggering inflammatory responses.

Furthermore, we observed H1N1-infected HRMECs using a microscope and found that cells exhibited distinct morphological features of death, cell rounding, and detachment. KEGG enrichment analysis of DEGs revealed a significant enrichment of the necroptosis pathway in H1N1 infection. Based on these observations, we hypothesize that necroptosis might play a major role in the cell death process of HRMECs after H1N1 infection. Similarly, previous study has also reported that influenza virus infection may lead to death of lung epithelial cells through necroptosis.[47]

The blood-retinal barrier consists of two distinct layers. The outer layer is primarily composed of retinal pigment epithelial cells and their tight junctions, whereas the inner layer is composed of retinal vascular endothelial cells and their tight junctions.[48,49] This barrier prevents substances from leaking out of the blood vessels and controls the entry and exit of immune cells. However, research has demonstrated that various conditions, such as ischemia, hypoxia, inflammation, infection, diabetes, and hypertension, can lead to the detriment of endothelial cells and subsequently disrupt the integrity of the blood-retinal barrie.[50] Homotypic interactions between endothelial cells help maintain vascular integrity, and the stability of blood vessels is crucial for maintaining the integrity of the blood-retinal barrie.[51,52] When cell adhesion is disrupted and abnormal connections occur between endothelial cells, blood vessels cannot maintain their stability, leading to increased vascular permeability and extensive leakage. Additionally, when the blood-retinal barrier is breached, numerous cytokines and chemokines recruit inflammatory cells, resulting in a strong inflammatory response.[53] Extensive retinal hemorrhage and inflammatory exudation have been observed in a significant number of patients infected with H1N1 influenza. In this in vitro study, RT-qPCR confirmed that various chemokines, cytokines, and genes related to IFN signaling pathways were significantly upregulated after HRMECs infection with H1N1. Excessive chemokines attract leukocytes and inflammatory cells to the sites of inflammation, leading to inflammation. Moreover, excess chemokines can increase intercellular gaps in endothelial cells and enhance vascular permeability, resulting in vascular leakage.[54] In contrast, the activation of IFN-related pathways can recruit inflammatory cells and enhance the inflammatory response. It can also enhance the killing effect of immune cells on endothelial cells, thereby disrupting the function of endothelial cells.[55] Our study revealed that HRMECs infection with H1N1 resulted in a significant upregulation of cytokines, chemokines, and genes related to IFN signaling pathways. The cells exhibited rounding, detachment, and apoptosis, which corresponded to the clinical manifestations of retinal hemorrhage and inflammatory exudation in patients. This preliminary study suggested possible reasons for the observed retinal manifestations in patients with H1N1 infection.

H1N1 infection activates the immune function of HRMECs, which produce a large number of inflammatory factors that exert defense and antiviral effects. These inflammatory factors play a protective role in the response to infection. However, if excessive inflammatory factors are not promptly cleared, they can over-activate the inflammatory response, disrupt the blood-retinal barrier, increase vascular permeability, and lead to leakage (Fig. 9). Studies have shown that antiviral drugs, such as oseltamivir, can effec-

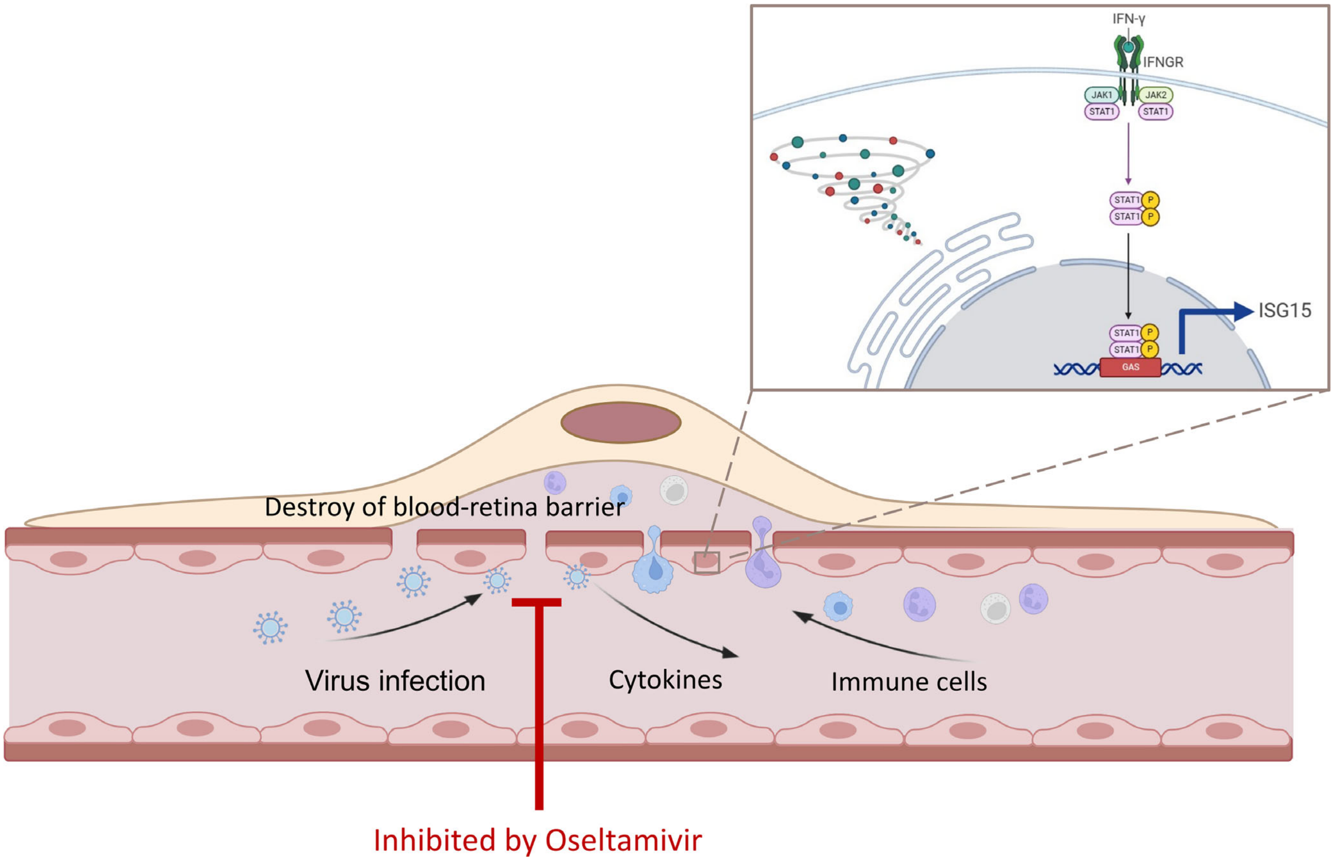

Figure 9. Underlying mechanisms of H1N1 infection in HRMECs causing inflammation and disruption of the blood-retinal barrier.

tively improve clinical symptoms caused by H1N1 viral infection. As illustrated in Figures 7A through 7O, we found that the upregulation of inflammatory factors induced by H1N1 infection in HRMECs showed a significant downward trend after intervention with oseltamivir and that the cellular condition improved significantly. Especially, the upregulation of CASP1 in the H1N1 infection group was significantly downregulated after oseltamivir treatment, indicating that oseltamivir might effectively suppress the expression of CASP1. CASP1 is an important member of the inflammasome complex that will be activated when the body infected.[56] The activation of CASP1 triggers the release of proinflammatory cytokines, participating in the regulation of inflammatory response.[57] This suggests that early intervention may reduce the risk of H1N1 infection–related retinal diseases. However, further research is needed to confirm this finding.

There are limitations of this study. We did not specifically knock down or overexpress the DEGs to validate the related specific mechanism. We will explore this issue further in future research. Furthermore, this study only conducted in vitro experiments and did not perform in vivo experiments, which is a limitation of this study. Our team intends to conduct animal experiments in the later stages to validate the conclusions derived from this experiment.

In conclusion, our study demonstrates for the first time that the H1N1 influenza virus can successfully infect HRMECs and replicate effectively within them. It is likely that the virus promotes an inflammatory response by upregulating the expression of chemokines and activating IFN-related signaling pathways, thereby inhibiting HRMECs proliferation and migration, and inducing HRMECs death, leading to the disruption of the blood-retinal barrier. Early intervention with oseltamivir in clinical practice has the potential to reduce retinal inflammation and hemorrhage in patients infected with H1N1.

Acknowledgments

Supported by grants (82271103) from the National Natural Science Foundation of China, a grant (2022A1515012326) from Guangdong Basic and Applied Basic Research Foundation, a grant (JCYJ20200109142418595) from Shenzhen Science and Technology Research and Development Foundation and a grant (BCF-KH-YK-20230803-08) from Bethune Charitable Foundation. The sponsors or funding organizations had no role in the design or conduct of this research; collection, management, analysis, and interpretation of the data; and preparation, review, or approval of the manuscript.

Disclosure: **S. Yang**, None; **Z. Fan**, None; **X. Lu**, None; **H. Liu**, None; **Z. Zhou**, None; **H. Qi**, None; **J. Zeng**, None; **M. Zheng**, None; **X. Zou**, None; **S. Fang**, None; **G. Zhang**, None

References

1. Benam KH, Denney L, Ho LP. How the respiratory epithelium senses and reacts to influenza virus. *Am J Respir Cell Mol Biol.* 2019;60:259–268.
2. Lycett SJ, Duchatel F, Digard P. A brief history of bird flu. *Philos Trans R Soc Lond B Biol Sci.* 2019;374(1775): 20180257.

3. Kobasa D, Takada A, Shinya K, et al. Enhanced virulence of influenza A viruses with the haemagglutinin of the 1918 pandemic virus. *Nature.* 2004;7099:703–707.
4. Park J-E, Ryu Y. Transmissibility and severity of influenza virus by subtype. *Infect Genet Evolution.* 2018;65:288–292.
5. Schanzer DL, Mosnier A, Caini S, et al. Clinical characteristics are similar across type A and B influenza virus infections. *Plos One.* 2015;10(9):e0136186.
6. Korteweg C, Gu J. Pandemic influenza A (H1N1) virus infection and avian influenza A (H5N1) virus infection: a comparative analysis. *Biochem Cell Biol.* 2010;88:575–587.
7. Kaji M, Watanabe A, Aizawa H. Differences in clinical features between influenza A H1N1, A H3N2, and B in adult patients. *Respirology.* 2003;8:231–233.
8. Mansour DEAA, El-Shazly AA-F, Elawamry AI, et al. Comparison of ocular findings in patients with H1N1 influenza infection versus patients receiving influenza vaccine during a pandemic. *Ophthalmic Res.* 2012;48:134–138.
9. Khairallah M, Kahloun R. Ocular manifestations of emerging infectious diseases. *Curr Opin Ophthalmol.* 2013;24:574–580.
10. Lai C-C, Chang Y-S, Li M-L, et al. Acute anterior uveitis and optic neuritis as ocular complications of influenza A infection in an 11-year-old boy. *J Pediatr Ophthalmol Strabismus.* 2011;48(6):30–3.
11. Michaelis M, Geiler J, Klassert D, et al. Infection of human retinal pigment epithelial cells with influenza A viruses. *Invest Ophthalmol Vis Sci.* 2009;50:5419–5425.
12. Fields MA, Del Priore LV, Adelman RA, et al. Interactions of the choroid, Bruch's membrane, retinal pigment epithelium, and neurosensory retina collaborate to form the outer blood-retinal-barrier. *Progr Retin Eye Res.* 2020;76:100803.
13. Stark R, Grzelak M, Hadfield J. RNA sequencing: the teenage years. *Nat Rev Genet.* 2019;20:631–656.
14. Grabherr MG, Haas BJ, Yassour M, et al. Full-length transcriptome assembly from RNA-Seq data without a reference genome. *Nat Biotechnol.* 2011;29:644–652.
15. Cegolon L, Salata C, Piccoli E, et al. In vitro antiviral activity of hypothiocyanite against A/H1N1/2009 pandemic influenza virus. *Int J Hyg Environ Health.* 2014;217:17–22.
16. Lei C, Yang J, Hu J, et al. On the calculation of TCID50 for quantitation of virus infectivity. *Virol Sin.* 2020;36:141–144.
17. Wiame I, Remy S, Swennen R, et al. Irreversible heat inactivation of DNase I without RNA degradation. *Biotechniques.* 2000;29:252–256.
18. Garson JA, Usher L, Al-Chalabi A, et al. Quantitative analysis of human endogenous retrovirus-K transcripts in postmortem premotor cortex fails to confirm elevated expression of HERV-K RNA in amyotrophic lateral sclerosis. *Acta Neuropathol Commun.* 2019;7(1):45.
19. Braun P, Gingras AC. History of protein–protein interactions: from egg-white to complex networks. *Proteomics.* 2012;12:1478–1498.
20. Szklarczyk D, Morris JH, Cook H, et al. The STRING database in 2017: quality-controlled protein–protein association networks, made broadly accessible. *Nucleic Acids Res.* 2017;45(D1):D362–D368.
21. Crisinel P-A, Barazzone C, Kaiser L, et al. Comparison of clinical presentation of respiratory tract infections in H1N1/09-positive and H1N1/09-negative patients. *Eur J Pediatr.* 2011;171:159–166.
22. Mu YP, Zhang ZY, Chen XR, et al. Clinical features, treatments and prognosis of the initial cases of pandemic influenza H1N1 2009 virus infection in Shanghai China. *QJM.* 2010;103:311–317.
23. Lopez-Prats MJ, Sanz Marco E, Hidalgo-Mora JJ, et al. Bleeding follicular conjunctivitis due to influenza H1N1 virus. *J Ophthalmol.* 2010;2010:1–2.
24. Jo T, Mizota A, Hatano N, et al. Frosted branch angiitis-like fundus following presumed influenza virus type A infection. *Jpn J Ophthalmol.* 2006;50:563–564.
25. Rifkin L, Schaal S. H1N1-associated Acute Retinitis. *Ocular Immunol Inflamm.* 2012;20:230–232.
26. Ito S-i, Takagi S, Takahashi M, et al. Bilateral retinitis after influenza virus infection in a case report. *Am J Ophthalmol Case Rep.* 2020;17:100584.
27. Turbeville SD, Cowan LD, Gass JDM. Acute macular neuroretinopathy—a review of the literature. *Surv Ophthalmol.* 2003;48(1):1–11.
28. Ashfaq I, Vrahimi M, Waugh S, et al. Acute macular neuroretinopathy associated with acute influenza virus infection. *Ocular Immunol Inflamm.* 2019;29:333–339.
29. Breker DA, Stacey AW, Srinivasan A, et al. Vision loss caused by retinal and lateral geniculate nucleus infarction in H1N1 influenza. *J Neuroophthalmol.* 2015;35:265–269.
30. Fajgenbaum DC, Longo DL, June CH. Cytokine storm. *N Engl J Med.* 2020;383:2255–2273.
31. Borish LC, Steinke JW. Cytokines and chemokines. *J Allergy Clin Immunol.* 2003;111(2):S460–S475.
32. Palomino DCT, Marti LC. Chemokines and immunity. *Einstein (São Paulo).* 2015;13:469–473.
33. Sokol CL, Luster AD. The chemokine system in innate immunity. *Cold Spring Harb Perspect Biol.* 2015;7(5):a016303.
34. Mei J, Liu Y, Dai N, et al. CXCL5 regulates chemokine scavenging and pulmonary host defense to bacterial infection. *Immunity.* 2010;33:106–117.
35. Antonelli A, Ferrari SM, Giuggioli D, et al. Chemokine (C–X–C motif) ligand (CXCL)10 in autoimmune diseases. *Autoimmun Rev.* 2014;13:272–280.
36. Callahan V, Hawks S, Crawford MA, et al. The pro-inflammatory chemokines CXCL9, CXCL10 and CXCL11 are upregulated following SARS-CoV-2 infection in an AKT-dependent manner. *Viruses.* 2021;13:1062.
37. Zeng Z, Lan T, Wei Y, et al. CCL5/CCR5 axis in human diseases and related treatments. *Genes Dis.* 2022;9:12–27.
38. Çelik N, Çelik O, Laloğlu E, et al. The CXCL9/10/11-CXCR3 axis as a predictor of COVID-19 progression: a prospective, case-control study. *Rev Soc Bras Med Trop.* 2023;56:e01282023.
39. Bonjardim CA. Interferons (IFNs) are key cytokines in both innate and adaptive antiviral immune responses—and viruses counteract IFN action. *Microbes Infect.* 2005;7:569–578.
40. Mesev EV, LeDesma RA, Ploss A. Decoding type I and III interferon signalling during viral infection. *Nat Microbiol.* 2019;4:914–924.
41. Randall RE, Goodbourn S. Interferons and viruses: an interplay between induction, signalling, antiviral responses and virus countermeasures. *J Gen Virol.* 2008;89:1–47.
42. Stark George R, Darnell James E. The JAK-STAT pathway at twenty. *Immunity.* 2012;36(4):503–514.
43. Negishi H, Taniguchi T, Yanai H. The interferon (IFN) class of cytokines and the IFN regulatory factor (IRF) transcription factor family. *Cold Spring Harb Perspect Biol.* 2018;10(11):a028423.
44. Satarker S, Tom AA, Shaji RA, et al. JAK-STAT pathway inhibition and their implications in COVID-19 therapy. *Postgrad Med.* 2020;133:489–507.
45. Tolomeo M, Cavalli A, Cascio A. STAT1 and its crucial role in the control of viral infections. *Int J Mol Sci.* 2022;23:4095.
46. Clark DN, Begg LR, Filiano AJ. Unique aspects of IFN-γ/STAT1 signaling in neurons. *Immunol Rev.* 2022;311:187–204.
47. Hong KS, Pagan K, Whalen W, et al. The role of glutathione reductase in influenza infection. *Am J Respir Cell Mol Biol.* 2022;67:438–445.

48. Yang X, Yu X-W, Zhang D-D, et al. Blood-retinal barrier as a converging pivot in understanding the initiation and development of retinal diseases. *Chin Med J.* 2020;133:2586–2594.
49. Yan Z, Wang C, Meng Z, et al. C1q/TNF-related protein 3 prevents diabetic retinopathy via AMPK-dependent stabilization of blood-retinal barrier tight junctions. *Cells.* 2022;11:779.
50. Vrints CJM, Krychtiuk KA, Van Craenenbroeck EM, et al. Endothelialitis plays a central role in the pathophysiology of severe COVID-19 and its cardiovascular complications. *Acta Cardiologica.* 2020;76:109–124.
51. Potente M, Gerhardt H, Carmeliet P. Basic and therapeutic aspects of angiogenesis. *Cell.* 2011;146:873–887.
52. Murdaca G, Colombo BM, Cagnati P, et al. Endothelial dysfunction in rheumatic autoimmune diseases. *Atherosclerosis.* 2012;224:309–317.
53. Giuffrida MJ, Valero N, Mosquera J, et al. Increased cytokine/chemokines in serum from asthmatic and non-asthmatic patients with viral respiratory infection. *Influenza Other Respir Viruses.* 2013;8:116–122.
54. Raz E, Mahabaleshwar H. Chemokine signaling in embryonic cell migration: a fisheye view. *Development.* 2009;136:1223–1229.
55. Dai J, Zhou P, Li S, et al. New insights into the crosstalk among the interferon and inflammatory signaling pathways in response to viral infections: defense or homeostasis. *Viruses.* 2022;14:2798.
56. Baena Carstens L, Campos D'amico R, Fernandes de Moura K, et al. Lung Inflammasome Activation in SARS-CoV-2 Post-Mortem Biopsies. *Int J Mol Sci.* 2022;23:13033.
57. Koraka P, Martina BEE, Smreczak M, et al. Inhibition of caspase-1 prolongs survival of mice infected with rabies virus. *Vaccine.* 2019;37:4681–4685.